NUCLEAR SCIENCE AND ENGINEERING: **181**, 48–59 (2015)

Automatic Mesh Adaptivity for Hybrid Monte Carlo/Deterministic Neutronics Modeling of Difficult Shielding Problems

Ahmad M. Ibrahim*

Oak Ridge National Laboratory, Reactor and Nuclear Systems Division
P.O. Box 2008, Building 5700, Oak Ridge, Tennessee 37831

Paul P. H. Wilson and Mohamed E. Sawan

University of Wisconsin–Madison, 1500 Engineering Drive, Madison, Wisconsin 53706

and

Scott W. Mosher, Douglas E. Peplow, John C. Wagner,
Thomas M. Evans, and Robert E. Grove

Oak Ridge National Laboratory, Reactor and Nuclear Systems Division
P.O. Box 2008, Building 5700, Oak Ridge, Tennessee 37831

Received August 12, 2014
Accepted December 27, 2014
http://dx.doi.org/10.13182/NSE14-94

Abstract—*The well-established Consistent Adjoint Driven Importance Sampling (CADIS) and the Forward Weighted Consistent Adjoint Driven Importance Sampling (FW-CADIS) hybrid Monte Carlo/deterministic techniques have dramatically increased the efficiency of neutronics simulations, yielding accurate solutions for increasingly complex problems through full-scale, high-fidelity simulations. However, for full-scale simulations of very large and geometrically complex nuclear energy systems, even the CADIS and FW-CADIS techniques can reach the CPU and memory limits of all but the very powerful supercomputers. In this work, three mesh adaptivity algorithms were developed to reduce the computational resource requirements of CADIS and FW-CADIS without sacrificing their efficiency improvements. First, a macromaterial approach was developed to enhance the fidelity of the deterministic models without changing the mesh. Second, a deterministic mesh refinement algorithm was developed to generate meshes that capture as much geometric detail as possible without exceeding a specified maximum number of mesh elements. Finally, a weight window (WW) coarsening (WWC) algorithm was developed to decouple the WW mesh and energy bins from the mesh and energy group structure of the deterministic calculations. By removing the memory constraint of the WW map from the resolution of the mesh and the energy group structure of the deterministic calculations, the WWC algorithm allows higher-fidelity deterministic calculations that, consequently, increase the efficiency and reliability of the CADIS and the FW-CADIS simulations. The three algorithms were used to enhance an FW-CADIS calculation of the prompt dose rate throughout the ITER experimental facility. Using these algorithms increased both the number of mesh tally elements in which nonzero results were obtained (+23.3%) and the overall efficiency of the calculation (a factor of >3.4). The three algorithms enabled this difficult calculation to be accurately solved using an FW-CADIS simulation on a 94-CPU computer cluster, eliminating the need for a world-class supercomputer.*

*E-mail: ibrahimam@ornl.gov

I. INTRODUCTION

Over the last decade, the role of neutronics modeling of reactor systems has been shifting from separate analyses of individual components to high-fidelity, full-scale analyses of entire systems. The high accuracy associated with minimizing modeling approximations by including more physical and geometric details is now feasible because of advancements in computing hardware and the development of efficient modeling methods. The Consistent Adjoint Driven Importance Sampling[1] (CADIS) and the Forward Weighted Consistent Adjoint Driven Importance Sampling[2] (FW-CADIS) hybrid Monte Carlo (MC)/deterministic techniques dramatically increase the efficiency of neutronics modeling and simulation, thus enabling accurate solutions for increasingly complex problems using high-fidelity, full-scale simulations of entire nuclear energy systems.[3] Both methods calculate the MC variance-reduction parameters using one or two relatively fast (low-resolution) deterministic calculations. The CADIS method is used to increase the efficiency of the MC calculations of localized quantities, while the FW-CADIS method is used to optimize multiple tallies that can be as extensive as mesh tallies covering the entire system.

The use of coarse meshes in CADIS and FW-CADIS simulations is necessary to speed up the deterministic calculations and decrease their memory requirements. Otherwise, high-fidelity, full-scale modeling of very large and geometrically complex nuclear energy systems would require unaffordable computing resources. The total number of mesh elements used in the deterministic calculations of CADIS and FW-CADIS simulations of very large and complicated problems can be $O(10^2)$ to $O(10^3)$ less than the total number of mesh elements required to model the problem for a deterministic-only solution.[4] Although the use of fine meshes increases both the efficiency and reliability of CADIS and FW-CADIS simulations,[4] it also increases the run time and memory requirements of the preliminary deterministic calculations and the memory requirements of the final MC calculation, which depend on the storage size of the variance-reduction parameters.

The goal of this work is to reduce the computational time and memory requirements of the CADIS and FW-CADIS methods while maintaining their dramatic efficiency improvements. Three automatic mesh adaptivity algorithms were developed and added to the AutomateD VAriaNce reducTion Generator (ADVANTG) code.[5] First, a macromaterial (MM) approach,[6] which mixes the materials for the deterministic calculations, enhances the fidelity of the deterministic models for a given spatial mesh. Second, a deterministic mesh refinement (DMR) algorithm improves the accuracy of structured mesh deterministic calculations by generating meshes that capture as much geometric detail as possible without exceeding a maximum number of mesh elements that is usually determined by the availability of computing resources. Finally, a weight window (WW) coarsening (WWC) algorithm decouples the mesh and energy group structure of the WW from the mesh and energy group structure of the deterministic calculations. This allows for a higher order of resolution in the deterministic mesh and for using data libraries with finer energy group structure without the burden of a correspondingly high-memory footprint for the WWs in the subsequent MC calculations.

All three algorithms were used to increase the efficiency of an FW-CADIS calculation of the prompt dose rate throughout the entire ITER experimental facility. This calculation represents a very challenging shielding problem because of the immense size (cylindrical model with a 34-m diameter and 25-m height) and complexity of the ITER structure and the presence of an optically thick (2-m) concrete biological shield.[7]

II. ALGORITHMS

II.A. Macromaterials

Automating the process of mapping the materials from the MC geometry to the deterministic mesh is necessary for CADIS and FW-CADIS simulations of problems with complex geometries. Previous implementations of CADIS and FW-CADIS deterministic calculations used a cell-center (CC) approach in which the material assigned to each mesh element in the deterministic model is based on the material at the center point of this element in the MC model. While this method is easily implemented and executes rapidly, it is difficult to capture important geometric detail using the CC approach. Furthermore, to decrease the computational and memory requirements of CADIS and FW-CADIS simulations, the mesh used in the deterministic calculations is generally coarser (tens of centimeters) than the mesh that would typically be used in a stand-alone discrete ordinates calculation. This increases the probability of "missing" important details in the deterministic calculations, which consequently decreases the efficiency and, in some cases, the reliability of the CADIS and FW-CADIS simulations.[4]

The MM approach[6] was developed to improve the discretized representation of the deterministic calculations of the SCALE (Ref. 8) MAVRIC shielding analysis sequence. It automatically creates a mixture for each mesh element in the deterministic model by homogenizing all of the materials that are contained within that mesh element in the MC model.

The steps of the MAVRIC MM approach can be summarized as follows:

1. Construct a subgrid over each of the user-supplied mesh elements. The number of subdivisions p in each dimension is supplied by the user. The total number of subelements is p^3.

2. Determine the material associated with each subelement using the CC approach.

3. Calculate approximate volume fractions (MM fractions) associated with each material in order to calculate a homogenized material mixture for each mesh element.

4. Loop through the newly created materials, and set materials with similar compositions, within a preset threshold, to be equivalent.

Because the materials are queried p^3 times in each mesh element, the error in approximating the volume fraction of materials, and thus the mass conservation, decreases as $O(1/p^3)$. The drawback of the MM approach is the potential creation of a large number of material mixtures. Step 4 is important for reducing the number of materials and hence minimizing the memory requirements; otherwise, the number of materials scales with the number of mesh elements in the original grid.

It is necessary to mention that the implementation of the MM approach in ADVANTG replaced the MAVRIC point-testing method with a ray-tracing technique that traces rays throughout the MC geometry. The starting points of rays are randomly sampled on the exterior $-X$, $-Y$, and $-Z$ faces of the deterministic mesh. Rays are then traced in the $+X$, $+Y$, and $+Z$ directions to the opposite side of the mesh. As each ray is traced, track length tallies record the length traced through each material in each mesh element. These track-length tallies are then used to estimate the MM fraction of each material within each mesh element.[9]

In addition to the improvement of the MC figure of merit (FOM) provided by the MM approach,[6] the DMR algorithm uses MM fractions of each mesh element. This is discussed in Sec. II.B.

II.B. Deterministic Mesh Refinement

In all previous implementations of CADIS and FW-CADIS, the positions of the planes of the deterministic structured mesh had to be manually chosen. Even with automation of the material specifications, developing an efficient mesh for the deterministic calculations can be difficult for large and complicated problems. The DMR algorithm was developed to create meshes that capture as much geometric detail as possible without exceeding a maximum number of mesh elements that is usually determined by the availability of computing resources.

The DMR algorithm uses a mesh potential function to describe the material heterogeneity in each mesh element. During the MM calculations, the constituents of each mesh element are internally stored in a vector of volume fractions. Each component in the vector represents the volume fraction of one of the materials in the MC model. The heterogeneity parameter used in developing the mesh potential function of the DMR algorithm is

$$h_{ijk} = (\sigma_{\max} - \sigma_{ijk}) V_{ijk} \ , \tag{1}$$

where

h_{ijk} = heterogeneity parameter of the mesh element defined by the three indices i, j, and k

σ_{ijk} = population standard deviation of the fractions in the vector consisting of the material fractions and the void fraction of the mesh element

$\sigma_{\max}$ = maximum possible standard deviation of this vector

V_{ijk} = volume of the element.

The maximum standard deviation $\sigma_{\max}$ of the materials vector corresponds to the standard deviation of mesh elements with only one material and no heterogeneities. This maximum standard deviation is defined in Eq. (2):

$$\sigma_{\max} = \frac{1}{\sqrt{N_{mat}}} \ , \tag{2}$$

where N_{mat} is the total number of materials in the MC model including vacuum. Because $\sigma_{\max}$ depends only on the number of materials in the original MC model, it does not depend on the fraction of each material in each mesh element. Theoretically, the standard deviation can be zero for cells with equal fractions of materials (including vacuum). These cells have the maximum disparity of materials and should have a high heterogeneity parameter. By subtracting the standard deviation from the maximum standard deviation, mesh elements with equal volumes will have maximum heterogeneity parameters if they have uniform material fractions and minimum heterogeneity parameters if they are composed of only one material. Table I shows a simple example of calculating $\sigma_{\max} - \sigma_{ijk}$ for four mesh elements with different materials fractions in an MC model with four materials including vacuum.

Like many discrete ordinates deterministic codes, Denovo (Ref. 10) performs calculations on an orthogonal, simply connected mesh in which each element face adjoins one and only one neighbor. Because Denovo is the deterministic code used by ADVANTG, the implementation of the mesh refinement algorithm in ADVANTG was constrained by preserving the connectivity of the orthogonal Cartesian mesh. A "block heterogeneity parameter" was defined for each X, Y, or Z block as the sum of the heterogeneity parameters of all of the elements that belong to each block:

$$H_i = \sum_{j,k} h_{ijk}, \quad H_j = \sum_{i,k} h_{ijk}, \quad H_k = \sum_{i,j} h_{ijk} \ . \tag{3}$$

Starting from a coarse user-defined initial mesh, the steps of the DMR algorithm can be summarized as follows:

TABLE I

Heterogeneity Parameter for Several Mesh Elements in a Model with Four Materials ($\sigma_{max} = 0.5$)

Materials/Cells	Element 1	Element 2	Element 3	Element 4
Vacuum	0.25	0.33	0.50	1.00
Material 1	0.25	0.33	0.50	0.00
Material 2	0.25	0.33	0.00	0.00
Material 3	0.25	0.00	0.00	0.00
Standard Deviations				
σ_{ijk}	0.00	0.17	0.29	0.50
$\sigma_{max} - \sigma_{ijk}$	0.50	0.33	0.21	0.00

1. Calculate the heterogeneity parameter of each mesh element using Eq. (1).

2. Calculate the block heterogeneity parameter of each X, Y, and Z block using Eq. (3).

3. Modify the mesh by inserting an extra plane at the midpoint between the two bounding planes of the X, Y, or Z block with the maximum heterogeneity parameter.

4. Recalculate the MM fractions and the heterogeneity parameter for each of the new elements added by the extra plane insertion.

5. Recalculate all block heterogeneity parameters.

6. Repeat steps 3, 4, and 5 until a user-specified total number of mesh elements is reached or until the sum of the heterogeneity parameters of all the mesh elements becomes zero.

For Cartesian meshes, the sum of the heterogeneity parameters of all the mesh elements can only be zero for underlying geometries with only rectangular cross-sectional areas. The maximum number of mesh elements is specified using a refinement parameter that represents the ratio between the total number of elements in the final and initial meshes.

II.C. Weight Window Coarsening

Both CADIS and FW-CADIS use deterministic adjoint fluxes to calculate a biased source and WW parameters for the MC calculation. The MC calculation cannot run if the MC code cannot allocate enough memory to store the WWs. Because the WWs are traditionally generated using the same mesh and energy group structure as the deterministic calculations, the size of the WW maps poses a very restrictive limit on the deterministic mesh resolution in CADIS and FW-CADIS simulations. Decoupling the WW and deterministic spatial and energy structures is necessary to allow the use of finer deterministic resolutions without increasing the storage size of the WW maps. An efficient algorithm for reducing the storage size of the WW maps should minimize the penalty in the MC efficiency that is expected because of the loss of fidelity as the WW map is coarsened.

The WWC algorithm uses a flux-weighted average of the adjoint fluxes, represented by

$$\phi^{+}_{IJK,G} = \frac{\sum_g \sum_{ijk} \phi^{+}_{ijk,g} \phi_{ijk,g} V_{ijk}}{\sum_g \sum_{ijk} \phi_{ijk,g} V_{ijk}} , \tag{4}$$

where

ijk, g = summations on the right side and include all of the fine space-energy elements that comprise the coarse space-energy element determined by the spatial indices I, J, and K and the energy group index G

V_{ijk} = volume of element ijk in the fine grid

$\phi_{ijk,g}, \phi^{+}_{ijk,g}$ = fluxes and adjoint fluxes of the fine grid.

While FW-CADIS uses forward and adjoint deterministic calculations, the CADIS method only requires an adjoint deterministic calculation. An extra forward deterministic calculation will be needed to apply the WWC algorithm for CADIS simulations.

By using a flux-weighted average of the adjoint flux, the adjoint flux of the coarse element is controlled by the adjoint fluxes of the fine elements with higher real (forward) fluxes. Furthermore, the adjoint fluxes calculated from Eq. (4) conserve the contributon flux,[11] represented by the forward flux multiplied by the adjoint flux, of the fine-mesh deterministic calculations.[a] Because the contributon flux identifies the potential response contribution of each region,[11] the coarse-mesh adjoint

[a]In this work, the contributon flux was approximated as the product of the scalar forward and adjoint fluxes. A quadrature integration of the angular moments can be used to improve the accuracy if the flux is strongly anisotropic.

flux, calculated by Eq. (4), preserves the expected response calculated using fine-mesh deterministic calculations.

In previous works, it has been theoretically proven[12] and demonstrated[4] that the CADIS and FW-CADIS methods populate the MC particles in phase-space proportional to the contributon flux. Space-energy regions with high contributon fluxes have a high population of MC simulated particles, and regions with low contributon fluxes have a low population of MC simulated particles. Therefore, regions with high contributon fluxes (high MC particle population) are expected to have a higher impact on increasing or decreasing the MC FOM in CADIS and FW-CADIS simulations than regions with lower contributon fluxes. The use of finer mesh and finer energy group structure reduces the deterministic discretization errors. This produces better WWs, which increase the MC FOM in CADIS and FW-CADIS simulations. To minimize the reduction in the MC FOM that is expected with the mesh coarsening necessary to reduce the size of the WW maps, it is desirable to preserve the fidelity of the mesh and the energy groups in the space-energy regions of highest contributon flux in CADIS and FW-CADIS simulations. Therefore, mesh elements with lower contributon fluxes should be collapsed (lose fidelity) before mesh elements with higher contributon fluxes.

Because only structured, simply connected WW maps can be used in MCNP (Ref. 13) without modification, removal of space-energy elements in ADVANTG WW maps was restricted to removal of spatial (X, Y, or Z) blocks or energy groups. The WWC algorithm used "block contributon parameters," representing the space and energy summations of the product of the contributon fluxes and volumes of all the space-energy elements belonging to each X, Y, or Z block or to each energy group:

$$C_i = \sum_g \sum_{j,k} \phi^+_{ijk,g} \phi_{ijk,g} V_{ijk} \ ,$$

$$C_j = \sum_g \sum_{i,k} \phi^+_{ijk,g} \phi_{ijk,g} V_{ijk} \ ,$$

$$C_k = \sum_g \sum_{i,j} \phi^+_{ijk,g} \phi_{ijk,g} V_{ijk} \ ,$$

$$C_g = \sum_{ijk} \phi^+_{ijk,g} \phi_{ijk,g} V_{ijk} \ . \tag{5}$$

The steps of the WWC algorithm can be summarized as follows:

1. Calculate the block contributon parameters for all blocks and energy groups.

2. Calculate the flux-weighted average adjoint fluxes [Eq. (4)] for all the space-energy elements of the spatial block or energy group with the lowest block contributon parameter ($C_{\min}$) and the corresponding space-energy elements of the neighboring block or energy group ($C_{neighbor}$).

3. Update the adjoint fluxes in all the space-energy elements of $C_{neighbor}$ by replacing them with the calculated average.

4. Update the forward fluxes and volumes of the space-energy elements of $C_{neighbor}$ by adding the corresponding forward fluxes and volumes of $C_{\min}$ to the corresponding values in $C_{neighbor}$. No volume changes will occur if $C_{\min}$ represents an energy group.

5. Update the block contributon parameter of $C_{neighbor}$ by adding the block contributon parameter of $C_{\min}$ to it.

6. Remove the forward and adjoint fluxes of all the space-energy elements of $C_{\min}$, and remove the block contributon parameter of $C_{\min}$.

7. Repeat steps 2 through 6 until the total number of space-energy elements reaches a user-specified value.

$C_{neighbor}$ should be the neighboring block or group with the lower block contributon parameter except for boundary blocks with only one neighbor. The user should determine the total number of space-energy elements in the final WW mesh to fit within the computer memory available for the MC calculations. The desired number of elements in the final WW map is specified using a collapsing parameter that represents the ratio of the total number of space-energy elements in the fine deterministic mesh to the total number of space-energy elements in the coarse WW mesh.

III. ITER PROMPT DOSE RATE

The three algorithms described in this work were applied to an FW-CADIS calculation of the ITER global prompt dose rate calculation described in Ref. 7. The goal of the analysis described in Ref. 7 was to emphasize the importance of the high-fidelity, full-scale modeling of large and complicated systems. In Ref. 7, it was shown that an accurate MC calculation of the prompt dose rate at a single point outside the biological shield (bioshield) would require about 400 processor·years using traditional variance-reduction techniques,[b] and the calculation of global prompt dose rates would be even more intractable. Because of the difficulty in completing such a calculation, previous assessments have depended on coupling the final three-dimensional (3-D) analysis with one- or two-dimensional analyses.[14] These approaches ignore critical geometric details—such as the effects of neutrons and photons streaming through the large diagnostics ports—and can overestimate the prompt dose rate by a factor of 100 or more.

[b]As described in Ref. 7, the single-tally MC calculation that did not employ the CADIS method used two traditional MCNP variance-reduction techniques, namely, a point-detector tally and implicit capture.

III.A. Methodology

The ITER 3-D model, Alite03 (Fig. 1), represents a 40-deg sector of the ITER device with reflecting boundaries in the toroidal direction.[15] The Alite03 model was created by using MCAM (Ref. 16), a CAD-MCNP interface program developed by the Fusion Design Study Team at the Institute of Plasma Physics, Hefei, China, to update the previously used BRAND model.[17] The MCNP5 input file for the Alite03 model exceeds 19 800 lines of geometry (cell and surfaces) description. Because of the geometric complexity, developing deterministic models that capture the geometric details of the Alite03 model is a very difficult process.

A Cartesian mesh tally with uniform cubic mesh elements with a side length of 10 cm was used to tally the total (neutron + photon) prompt operational dose rates throughout the entire portion of the ITER experimental facility covered by the Alite03 model.

ADVANTG was used to employ the FW-CADIS method for this analysis. Source biasing was not used. Because the source particles are emitted in vacuum with a very narrow Gaussian energy distribution with a mean value of 14.1 MeV, the biasing parameters change very little, less than an order of magnitude, over the volume in which the source is emitted. To optimize the mesh tally, the adjoint source in ADVANTG was defined to include all of the ITER geometry. The groupwise energy spectrum of the adjoint source was defined as the flux–to–dose rate conversion factors in an energy structure equivalent to that of the multigroup data library of the deterministic calculation.

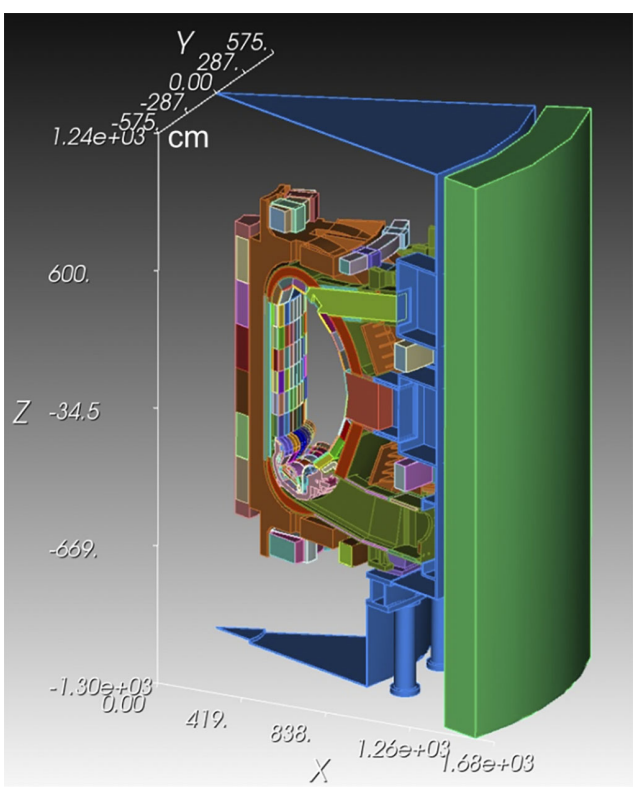

Fig. 1. The ITER MC model Alite03.

For the forward and adjoint Denovo calculations to be performed within the limited computing resources (32 processors with ~1 Gbyte per processor), the number of mesh elements in all of the Denovo calculations was set to not exceed eight million cells. A uniform cubic mesh with a side length of 16.36 cm was used. For this uniform mesh, both the CC and the MM approaches were used for the material definitions in two different FW-CADIS cases. The DMR algorithm was also used to automatically create a mesh with the same total number of mesh elements. An initial mesh with 1.3×10^6 elements was used for the automatically refined case. This initial mesh had uniform side lengths of 32.7 cm in the Y direction and 35.3 cm in the Z direction. The initial dimensions of the mesh elements were varied in the X direction to capture the flux gradient in the bioshield and the inner shielding layers. After the final mesh was automatically generated using the DMR algorithm, the MM approach was used for the material definitions in the Denovo model. The WWC algorithm was also used to collapse the fluxes of the automatically refined FW-CADIS case by factors of 2, 4, 8, 16, and 32.

A 46 neutron/21 gamma group FENDL 2.1 library[18] was used for the Denovo calculations, and a continuous-energy FENDL 2.1 library was used for the MCNP calculation.

III.B. Effects of MMs and DMR

A common approach to analyze the efficiency of MC calculations of mesh tally distributions is to measure the fraction of elements having a relative uncertainty less than some prescribed value at a fixed wall-clock time. The cumulative distribution functions (CDFs) of mesh tally uncertainties at a fixed wall-clock time have frequently been used for this purpose.[2,19] The CDF for a perfectly converged MC solution would have a sharp jump to 100% of the mesh elements near a relative uncertainty $R = 0$, indicating uniformly well-converged tallies. Figure 2 shows the CDFs of the mesh tally relative uncertainties R for an analog MC calculation and for the three FW-CADIS cases that did not use WWC. The MCNP running time was fixed at 10 processor·days for each of the four cases in Fig. 2. All of the cases used the serial MCNP5 version to avoid distorting the efficiency analysis with the times spent by the scheduling and the communication processes of parallel MCNP5.

As demonstrated in Fig. 2, only 15% of the mesh tally elements in the analog case achieved an R of $<100\%$, indicating that 85% of the elements did not score a single event in a 10-day computation. In contrast, between 93% and 98% of all elements in all the FW-CADIS cases had

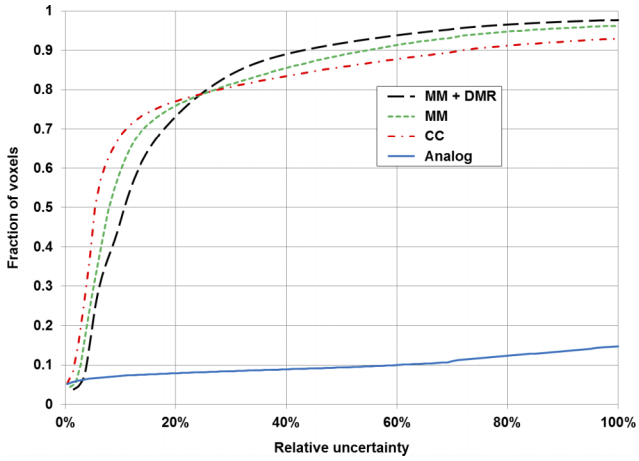

Fig. 2. Cumulative distribution functions of mesh tally relative uncertainties for 10-day MC calculations of analog MC case and three FW-CADIS cases.

at least one scoring event. Also, from Fig. 2, it is apparent that >70% of all of the elements in each FW-CADIS case obtained an R below 20%, and nearly 50% to 70% of the elements in these cases obtained relative uncertainties of 10% or less. Based on these preliminary calculations, the minimum MCNP computer time required to reduce the relative uncertainty of 90% of the tallies to below 10% for any of the FW-CADIS simulations is about 190 processor·days.

Table II shows the computer time utilized in performing the deterministic calculations (forward and adjoint) for the three FW-CADIS cases. The initialization times include the time spent in generating the Denovo models for the FW-CADIS calculations.

The adjoint Denovo calculation for the FW-CADIS case that used the MM approach but did not use the DMR algorithm took 56.85 processor·days, which is at least a factor of 9.1 longer than any of the other Denovo calculations with the same number of elements. For some of the Denovo routines in this calculation, the differences in the time fractions at which the processors were occupied by performing the actual calculations exceeded one order of magnitude. This indicates that the unusually long computational time of this calculation was caused by the hard disk swapping that occurs when a computational node on a UNIX computational cluster runs out of memory. To avoid this dramatic effect of hard disk swapping, the memory requirement of each subspace associated with each parallel process in the Denovo calculation must be carefully computed before starting the calculation. Further attention is needed with the MM approach because the scattering matrix of a certain subspace may require a substantial amount of memory if it includes a very large number of mixed materials. Without the hard disk swapping effect, both the deterministic and initialization times will be relatively small compared to the computer time required by a more accurate MCNP calculation, which exceeds 190 processor·days. For initialization times of the MM case with no mesh refinement and the automatic mesh refinement case to be comparable, the MM parameter used for the MM case with no mesh refinement was set to be 5, and the MM parameter of the automatic mesh refinement case was set to be 3.

Table III shows the fraction of the mesh tally elements that had MC scoring and the FOMs defined for the three FW-CADIS cases. The FOMs in Table III are based on the average relative variance, a metric often used in assessing the efficiency of global MC problems.[20] This FOM is defined as

$$\mathrm{FOM} = \frac{1}{\overline{R^2}T} \ , \tag{6}$$

where $\overline{R^2}$ is the mean of the distribution function of the relative variances (R^2) of the mesh tally elements and T is the MC computation time. In Ref. 20, the basic assumption for this FOM was that the user desires as many mesh tally elements to have R below a specific value for the shortest time possible. In MC calculations of large and complicated problems such as the calculation of the dose rate everywhere throughout an entire nuclear facility, the calculations frequently will be stopped before MC scoring occurs in all the mesh tally elements because it is usually practically impossible to score in all the mesh tally elements for these kinds of problems. A typical procedure for calculating $\overline{R^2}$ is to assign $R = 100\%$ for all the elements without MC scoring. The FOM is expected

TABLE II

Computational Time of Three FW-CADIS Cases

	Time (processor·h)	
Case	Initialization	Deterministic
CC	0.6	195.2
MM	16.6	1514.7
MM + DMR	14.1	222.6

TABLE III

Monte Carlo FOM and Fraction of Mesh Tally Elements with MC Scoring for Three FW-CADIS Cases for ITER Prompt Dose Rate Problem

Case	Fraction of Nonzero Elements (%)	Normalized FOM
CC	95.5	7.2
MM	97.5	9.1
MM + DMR	98.3	11.1

to be overestimated with this assumption because elements with no MC scoring are expected to have a slower convergence rate than the tallies with $R = 100\%$. The magnitude of the overestimation in this FOM is expected to be lower for the cases with larger fractions of nonzero scoring elements. Therefore, an MC calculation with a higher FOM is not necessarily more efficient than an MC calculation with a lower FOM if the low FOM MC calculation has a higher fraction of nonzero scoring elements. However, an MC calculation with a higher FOM and a higher fraction of nonzero scoring elements is much more likely to be more efficient than an MC calculation with a lower FOM and a lower fraction of nonzero elements because the high FOM MC calculation will have a lower overestimation in its high FOM. In this analysis, the FOMs were normalized by dividing them by the FOM calculated for the analog case, and the Rs of the zero scoring mesh tally elements were considered to be 100%. Each normalized FOM in isolation does not signify the efficiency of the FW-CADIS calculation compared to the analog calculation because of the meaningless highly overestimated value of the analog FOM where ~85% of the mesh tally elements do not have scoring; however, comparing the different FOMs of the FW-CADIS cases is useful in assessing their efficiencies.

The use of the MM approach in creating the deterministic models increased the fraction of elements with MC scoring by 2.1% (53 000 elements), and using the MM approach along with the DMR algorithm increased the fraction of elements with MC scoring by 2.9% (74 000 elements). Additionally, the FOM of the MM case is 26.4% higher than the CC case, and the FOM of the third case that applied both the MM and the DMR algorithms is 54.2% higher than the CC case.

The calculated dose rates on the central plane of ITER and on a plane rotated 20 deg from the central plane are shown in Fig. 3 for the three FW-CADIS cases. The third case, which applied both the MM and the DMR algorithms, had more mesh tally elements with MC scoring in the upper diagnostics port, which is plugged by 5 m of shielding materials, and in the equatorial port, which is plugged by 2 m of shielding materials. Because it is difficult for MC particles to score in the shielding plugs of these ports, the extra scoring in these regions shows that the WW parameters of the third case are more effective than the CC and MM cases.

III.C. Effects of WWC

Table IV shows the fraction of scoring elements and global MC FOM for 10-day MCNP runs of the FW-CADIS case that used both the MM approach and the DMR algorithm and the five FW-CADIS cases that used the WWC algorithm to reduce the size of the WW map of the automatically refined FW-CADIS case by factors of 2, 4, 8, 16, and 32, respectively. The FOMs were calculated using Eq. (6) and normalized to the analog FOM values. The Rs of the zero scoring elements were considered to be 100%. The computational time spent in the WWC algorithm was <20 h for each case. The goal of this preliminary analysis is to determine the FW-CADIS WW map that can be used with an MC calculation that will be run for hundreds of processor·days. The time spent in the WWC algorithm was not included in the FOM analysis

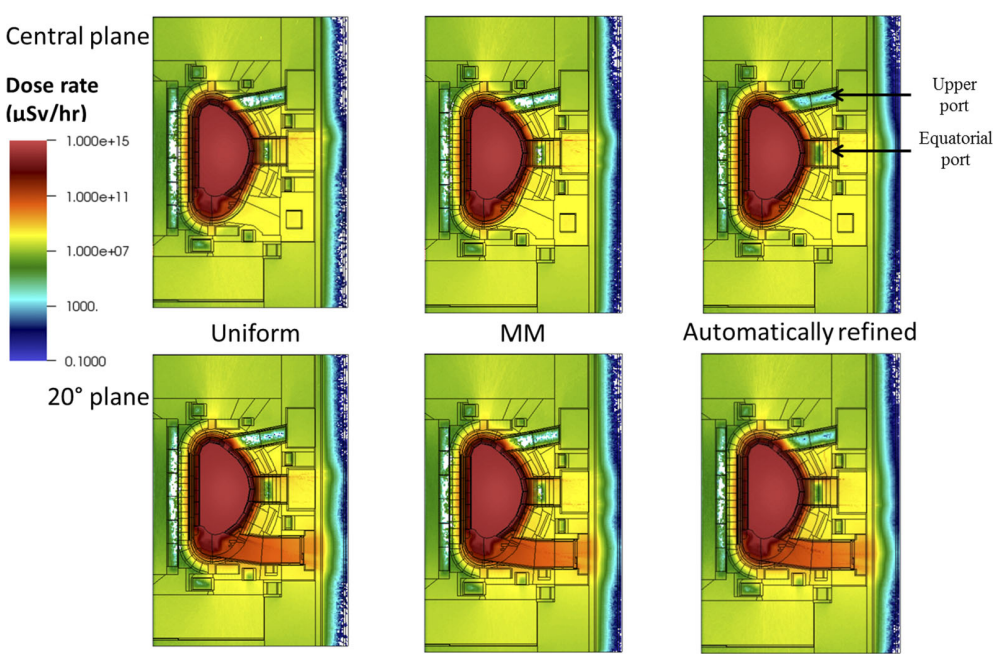

Fig. 3. Dose rate map on central plane and on plane rotated 20 deg from central plane for three FW-CADIS cases.

TABLE IV

Monte Carlo FOM and Fraction of Mesh Tally Elements with MC Scoring for FW-CADIS Cases with WWC

Case	Size of WW File (Gbyte)	Fraction of Nonzero Elements (%)	Normalized FOM
No coarsening	6.5	98.3	11.1
Coarsening 2	3.3	98.3	11.2
Coarsening 4	1.7	97.8	9.0
Coarsening 8	0.8	97.5	8.2
Coarsening 16	0.4	97.6	9.7
Coarsening 32	0.2	97.8	10.1

because the amount of time needed by the actual MC simulation to obtain statistically relevant answers is large (on the order of hundreds of days) compared to the time spent generating a reduced-size WW map.

For all of the cases with the reduced-size WW maps, the decrease in the fraction of nonzero scoring mesh tally elements was $<1\%$, and the decrease in the MC FOM was $<26.1\%$. Between the original case with no coarsening and the case that used the WWC algorithm to decrease the storage size of the WW map by a factor of 32, the reduction in the fraction of elements with calculated MC results was only 0.5%, and the reduction in the FOM was only 9%. These reductions in the MC efficiency are offset and easily justified by the large compensatory reduction in the size of the WW map, which in turn greatly facilitates the ability to employ parallel processing in the MC calculation.

III.D. Combined Effect of MMs, DMR, and WWC

As noted in Sec. III.B, even with the FW-CADIS method, an accurate and reliable MCNP calculation of a problem with the magnitude and complexity of this system requires hundreds of processor·days. Performing such a calculation without parallel processing is difficult. Because the size of the WW map may constitute the limiting factor on the number of MCNP jobs that can be run in parallel, it is illustrative to compare the MC efficiencies of different FW-CADIS cases with similar WW map sizes.

Figure 4 shows the CDFs of the mesh tally R for two 10-day MCNP runs. Each of these two MCNP runs used a different combination of FW-CADIS options; however, both used similarly sized WW maps that occupied ~ 0.21 Gbyte of hard disk space.

The first FW-CADIS case did not use any of the algorithms developed in this work and used the CC approach for defining the materials in the deterministic calculations. The Denovo model for this case used a

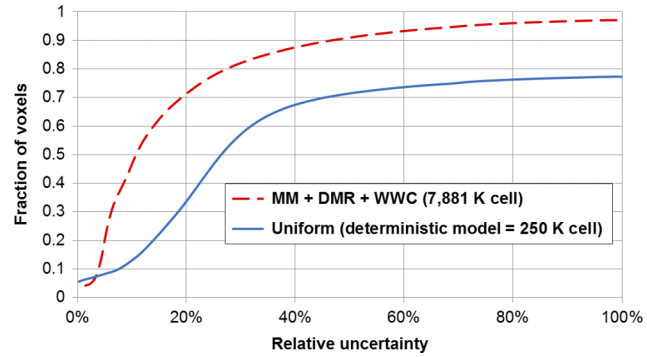

Fig. 4. Cumulative distribution functions of mesh tally relative uncertainties for 10-day MC calculation of FW-CADIS cases with 0.206-Gbyte WW map.

uniform mesh for which the elements had side lengths of between 40 and 42.33 cm. The total number of space-energy elements in the Denovo model for this case was 16.4×10^6. The second FW-CADIS case used the same automatically refined Denovo model created for the automatic refinement case of Sec. III.B. This Denovo model contained 528.0×10^6 space-energy elements. The WWC algorithm was used to reduce the number of space-energy elements in the WW map of this case to 16.3×10^6.

Table V shows the fraction of nonzero scoring mesh tally elements and the MC FOM of the two FW-CADIS cases. The FOMs were calculated using Eq. (6) and normalized to the analog FOM values. The Rs of the zero scoring mesh tally elements were considered to be 100%.

For the FW-CADIS cases with WW maps occupying ~ 0.21 Gbyte of hard disk space, using the three algorithms provided a 23.3% increase in the fraction of the nonzero scoring mesh tally elements (2 676 552 elements) and a factor of 3.4 increase in the MC FOM. The global FOM calculated using Eq. (6) is overestimated, but the magnitude of the overestimation is proportional to the number of elements for which the Rs of the zero scoring mesh tally elements were replaced by 100%. Because the FW-CADIS case that used the three algorithms had 23.3% more nonzero scoring elements than the FW-CADIS case that did not use any of the

TABLE V

Fraction of Mesh Tally Elements with Scoring and the MC FOM of Two FW-CADIS Cases with 0.206-Gbyte WW Map for ITER Prompt Dose Rate Problem

Case	Fraction of Nonzero Elements (%)	Normalized FOM
No adaptivity	79.3	3.0
Adaptivity	97.8	10.1

algorithms, the improvement in the real (asymptotic) MC FOM is expected to be higher than the calculated value. As will be shown in Sec. III.E, this substantial enhancement in the MC FOM, which significantly reduces the calculation time, enables accurate MC simulation for this very difficult problem using affordable computing resources.

III.E. Global Prompt Dose Rate Calculation with Parallel Processing

The combined effect of the three algorithms developed in this work enabled performing a 940-processor-day, FW-CADIS accelerated MCNP calculation with parallel processing on the UNIX computer cluster of the University of Wisconsin–Madison Department of Engineering Physics. For this calculation, 92.7% of the mesh tally elements had relative uncertainties $< 10\%$. Of all of the mesh tally elements (2 676 552) that lie within the 40-deg sector of the MCNP model, only 19 elements did not have MC scoring in this calculation. Figure 5 shows the results of this calculation that represent the dose rate map on the central plane of the model and on a plane rotated 20 deg from the central plane.

To develop confidence in the accuracy of this FW-CADIS calculation, the global MC results at four points were compared to the results of two other approaches. The four points represent interesting positions inside and outside the bioshield at the midplane and at the bottom of the tokamak. The positions of the four points used in the verification of the global MC calculation are shown in Fig. 6.

The results of the global MC calculation at these four points were compared to results from an MC calculation using four point detectors (F5 tallies) at the four positions. This calculation used the FW-CADIS method with four point adjoint sources having an energy spectrum equal to the flux–to–dose rate conversion factors in the 46 neutron/21 gamma energy group structure of the multigroup library used in the deterministic calculation. It was necessary to use the FW-CADIS method for this calculation because the computer time required for doing such a calculation using conventional MC simulations is too large. However, the calculation still provided some complementarity from the original global FW-CADIS calculation because the convergence of the MC calculations is much faster when the FW-CADIS method is used to optimize only localized tallies. Using the next event estimator of the point-detector tally instead of the track length estimator of the mesh tally provided another type of complementarity between the two calculations. The dose rates at these four positions were also compared to the dose rates calculated deterministically with a standalone Denovo calculation that used a spatial mesh with 1.34 billion elements, a 46 neutron/21 gamma energy group FENDL2.1 cross-section library, and 1.6×10^{15} total unknowns. This high-performance-computing (HPC) calculation was performed on 33 552 cores of the Oak Ridge National Laboratory supercomputer Titan. ADVANTG was used to create the input file for this HPC Denovo calculation. An approximate source that peaked in the plasma zone was used to approximate the ITER source. Table VI shows the dose rates calculated at the four points using the mesh tally, the point detectors, and the HPC Denovo calculations.

Considering the 13 to 14 orders-of-magnitude attenuation between the source region and points 2 and 4 as well

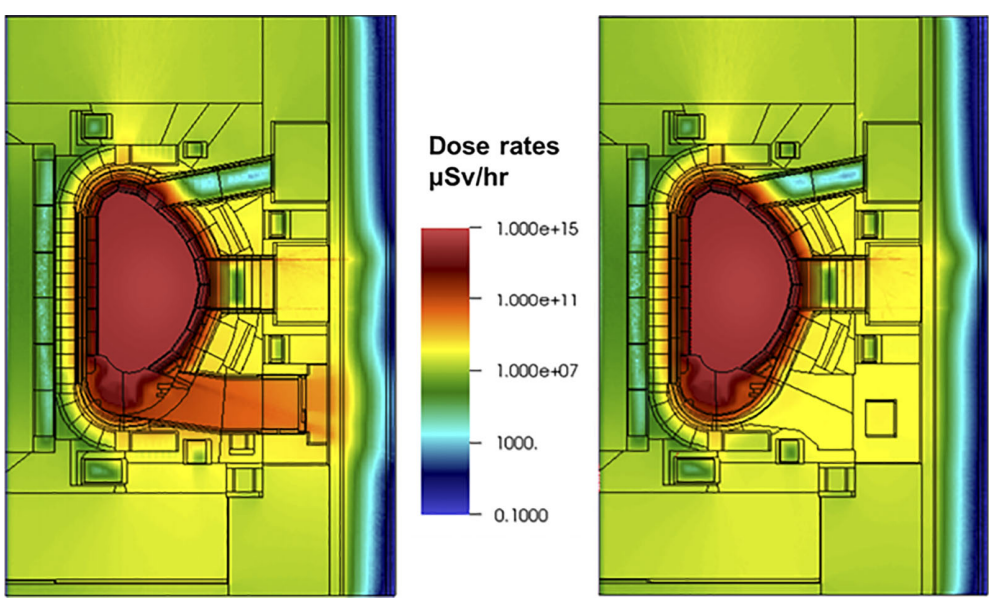

Fig. 5. Dose rate map on central plane and on plane rotated 20 deg from central plane for 940 days of MCNP runs with FW-CADIS and three algorithms.

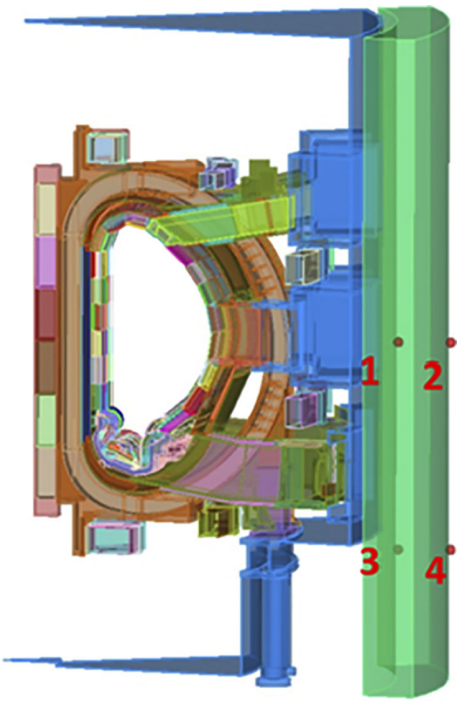

Fig. 6. Positions of the four points used in validation of ITER prompt dose rate global MC calculation.

as the 7 to 8 orders-of-magnitude attenuation between the source and points 1 and 3, the global MC results showed very good agreement with both the point-detector and the HPC Denovo results. The maximum relative difference between the point-detector results and the global MC results is 40.0%, while the maximum relative difference between the global MC results and the Denovo results is 35.7%. Additionally, portions of these differences are expected because the global MC results are averaged across cubic mesh elements with sides of 10 cm, the Denovo results are averaged across cubic mesh elements with sides of 2 cm, and the point-detector results are not averaged.

IV. CONCLUSION

To increase the fidelity of the deterministic calculations used in CADIS and FW-CADIS simulations without exceeding a total number of mesh elements—which can be determined by the limits of available computing resources—the MM approach and the DMR algorithm were developed. The MM approach provides a method for homogenizing the materials of each mesh element in the deterministic models. For a fixed number of mesh elements, the DMR algorithm seeks an efficient mesh that can reduce the geometry discretization errors that are inevitable with the use of structured mesh deterministic calculations to generate the variance-reduction parameters in CADIS and FW-CADIS simulations of large and geometrically complex problems. The algorithm makes it much easier for the user to develop an appropriate, problem-dependent mesh for the deterministic calculations of the CADIS and FW-CADIS simulations. By increasing the fidelity of the deterministic models, the MM and the DMR algorithms are found to generally increase both the accuracy of the deterministic solutions and the efficiency of the MC calculations in CADIS and FW-CADIS simulations.

Using finer mesh resolution is desirable for CADIS and FW-CADIS simulations because it reduces both the truncation and the geometry discretization errors of the deterministic calculations and consequently increases the CADIS and FW-CADIS simulation efficiency. Because of the one-to-one correspondence of the spatial mesh and energy groups between the deterministic solution and the WW map in the previous implementations of CADIS and FW-CADIS simulations, the deterministic mesh resolution was limited not just by the availability of computing resources but also by the size of the WW maps generated for the MC calculations. This latter limitation can be very restrictive with parallel processing because current production-level MC codes (e.g., MCNP5) depend on replication of the MC data (geometry, cross sections, WW parameters, etc.). Development and use of a WWC algorithm alleviates this restrictive limitation. The WWC algorithm uses a flux-weighted average of the adjoint fluxes to decouple the space-energy mesh of the WW maps from the mesh and energy group structure of the deterministic calculations. This flux-weighted average conserves the deterministic estimate of the MC particles as represented by the contributon flux, which was approximated by the product of the space- and energy-dependent scalar forward and adjoint fluxes of each space-energy cell. By conserving the contributon fluxes of the deterministic calculations, the weights generated by

TABLE VI

Dose Rates Calculated at Four Points for ITER Global Prompt Dose Rate Problem

Points	Mesh Tally (μSv/h)	Point Detector (μSv/h)	Denovo (μSv/h)
1	$2.0 \times 10^7 \pm 7.0\%$	$2.8 \times 10^7 \pm 5.5\%$	2.2×10^7
2	$17 \pm 6.3\%$	$15 \pm 4.4\%$	14.2
3	$4.2 \times 10^6 \pm 0.6\%$	$5.3 \times 10^6 \pm 2.1\%$	4×10^6
4	$2.8 \pm 14.0\%$	$2.3 \pm 2.8\%$	1.8

the adjoint flux collapsing formula are controlled by the weights of the collapsed mesh elements with higher fluxes. Additionally, the WWC algorithm carefully distinguishes the space-energy cells with the fewest MC particles (smallest contributon flux) from those of greater importance and selectively removes them from the data to be processed in order to reduce the computer memory burden. This minimizes the reduction in the MC FOM that is expected with any averaging scheme because of the inevitable loss of fidelity in the WW map.

The three algorithms developed in this work were used in calculating the prompt dose rate throughout the portion of the ITER experimental facility described in the Alite03 model. This calculation represents a very challenging shielding problem because of the immense size and complexity of the ITER structure and the presence of a 2-m bioshield. Compared to an FW-CADIS calculation with the same storage size of the variance-reduction parameters, the use of the three algorithms increased the regions for which nonzero MC results were achieved by 23.3% and increased the efficiency of the MC calculation by a factor of 3.4 for a 10-day MCNP calculation. Because of significant improvement in the MC efficiency without any increase in the memory requirement, the use of the three algorithms with FW-CADIS enabled the simulation of this difficult shielding problem on the University of Wisconsin–Madison Department of Engineering Physics computer cluster using parallel processing for the MC calculations.

ACKNOWLEDGMENTS

This manuscript has been authored by UT-Battelle, LLC, under contract DE-AC05-00OR22725 with the U.S. Department of Energy.

REFERENCES

1. J. C. WAGNER and A. HAGHIGHAT, "Automated Variance Reduction of Monte Carlo Shielding Calculations Using the Discrete Ordinates Adjoint Function," *Nucl. Sci. Eng.*, **128**, 186 (1998); http://dx.doi.org/10.13182/NSE98-2.

2. J. C. WAGNER, D. E. PEPLOW, and S. W. MOSHER, "FW-CADIS Method for Global and Regional Variance Reduction of Monte Carlo Radiation Transport Calculations," *Nucl. Sci. Eng.*, **176**, 37 (2014); http://dx.doi.org/10.13182/NSE12-33.

3. J. C. WAGNER et al., "Review of Hybrid (Deterministic/Monte Carlo) Radiation Transport Methods, Codes, and Applications at Oak Ridge National Laboratory," *Prog. Nucl. Sci. Technol.*, **2**, 808 (2011).

4. A. M. IBRAHIM, "Automatic Mesh Adaptivity for Hybrid Monte Carlo/Deterministic Modeling of Difficult Shielding Problems," PhD Thesis, University of Wisconsin–Madison (2012).

5. S. W. MOSHER et al., "Automated Weight-Window Generation for Threat Detection Applications Using ADVANTG," *Proc. Int. Conf. Mathematics, Computational Methods and Reactor Physics (M&C 2009)*, Saratoga Springs, New York, May 3–7, 2009, American Nuclear Society (2009).

6. A. M. IBRAHIM et al., "Improving the Mesh Generation Capabilities in the SCALE Hybrid Shielding Analysis Sequence," *Trans. Am. Nucl. Soc.*, **100**, 302 (2009).

7. A. M. IBRAHIM et al., "Global Evaluation of Prompt Dose Rates in ITER Using Hybrid Monte Carlo/Deterministic Techniques," *Fusion Sci. Technol.*, **60**, 676 (2011); http://dx.doi.org/10.13182/FST10-292.

8. S. M. BOWMAN, "SCALE 6: Comprehensive Nuclear Safety Analysis Code System," *Nucl. Technol.*, **174**, 126 (2011); http://dx.doi.org/10.13182/NT10-163.

9. S. R. JOHNSON, "Fast Mix Table Construction for Material Discretization," *Proc. Int. Conf. Advances in Mathematics, Computational Methods, and Reactor Physics*, Sun Valley, Idaho, May 5–9, 2013, p. 571, American Nuclear Society (2013).

10. T. M. EVANS et al., "Denovo: A New Three-Dimensional Parallel Discrete Ordinates Code in SCALE," *Nucl. Technol.*, **171**, 171 (2010); http://dx.doi.org/10.13182/NT10-5.

11. M. L. WILLIAMS, "Generalized Contributon Response Theory," *Nucl. Sci. Eng.*, **108**, 355 (1991); http://dx.doi.org/10.13182/NSE90-33.

12. T. BECKER, "Hybrid Monte Carlo/Deterministic Methods for Radiation Shielding Problems," PhD Thesis, University of Michigan (2009).

13. X-5 MONTE CARLO TEAM, "MCNP—A General N-Particle Transport Code, Version 5—Volume I: Overview and Theory," LA-UR-03-1987, Los Alamos National Laboratory (2003).

14. H. IIDA et al., "Nuclear Analysis Report," Version 2, ITER IDM G 73 DDD 2 W 0.2, ITER (July 2004).

15. M. J. LOUGHLIN et al., "ITER Nuclear Analysis Strategy and Requirements," *Fusion Sci. Technol.*, **56**, 566 (2009); http://dx.doi.org/10.13182/FST09-19.

16. S. SATO, "Development of a CAD/MCNP Interface Program Prototype for Fusion Reactor Nuclear Analysis," *Fusion Eng. Des.*, **81**, 2767 (2006); http://dx.doi.org/10.1016/j.fusengdes.2006.07.070.

17. H. IIDA, "Fast Neutron Flux and Nuclear Heat in the TF Coil Inboard Legs vs. Gap Width Among Blanket. NAG-236," ITER International Organization (2003).

18. D. L. ALDAMA and A. TRKOV, "FENDL2.1, Update of an Evaluated Nuclear Data Library for Fusion Applications," INDC (NDS) 467, International Atomic Energy Agency (2004).

19. D. PEPLOW, "Comparison of Hybrid Methods for Global Variance Reduction in Shielding Calculations," *Proc. Int. Conf. Advances in Mathematics, Computational Methods, and Reactor Physics*, Sun Valley, Idaho, May 5–9, 2013, p. 231, American Nuclear Society (2013).

20. B. C. KIEDROWSKI and A. M. IBRAHIM, "Evaluating the Efficiency of Estimating Numerous Monte Carlo Tallies," *Trans. Am. Nucl. Soc.*, **104**, 325 (2011).